Step-like displacements of a deep seated gravitational slope deformation observed during the 2016–2017 seismic events in Central Italy

"STEP-LIKE DISPLACEMENT OF A DEEP SEATED GRAVITATIONAL SLOPE DEFORMATION OBSERVED DURING THE 2016-2017 SEISMIC EVENTS IN CENTRAL ITALY"

Gabriele Amato [1], Roberto Devoti [2], Giandomenico Fubelli [3], Domenico Aringoli [4], Christian Bignami [2], Alessandro Galvani [2], Marco Moro [2], Marco Polcari [2], Michele Saroli [5, 2], Vincenzo Sepe [2], Salvatore Stramondo [2]

[1] Department of Sciences - Roma Tre University, Roma (Italy); [2] INGV - Istituto Nazionale di Geofisica e Vulcanologia, Roma; [3] University of Turin, Turin (Italy); [4] School of Sciences and Technology - University of Camerino, Camerino (Italy); [5] Department of Civil and Mechanical Engineering - University of Cassino and Southern Lazio, Cassino (Italy).

Abstract

Deep Seated Gravitational Slope Deformations are characterized by low deformation rates although they can experience partial-collapse phases or more rapid movements, especially in presence of active tectonic structures. In the Central Italy, considering the high seismicity rate, seismic activity must be considered to be an important trigger of deep slope movements. We aim to contribute to the research in this field by reporting the results of a monitoring program on a Deep Seated Gravitational Slope Deformation in this region that involves marly calcareous rocks. We documented the pre-seismic evolution of the phenomenon and measured its seismically induced displacements during the earthquake sequence in 2016 and 2017 in Central Italy, which largest events were magnitude 5.0-to-6.5.

A multidisciplinary approach that combines a field geomorphological survey, installation of permanent GPS stations, and InSAR elaborations was adopted for this study.

The average ground motion rate of the slope deformation before the earthquakes was very low (<3 mm/y) and not spatially homogenous, as detected by GPS and InSAR. In detail, the uppermost area of the slope instability likely moves faster than the lowest sector.

On the other hand, GPS and InSAR recorded significant step-like movements, one to ten times higher than the normal activity rate, triggered by the magnitude 5.0-to-6.5 earthquakes. In detail, the movement mainly depended on the magnitude of the earthquake and the distance from the epicenter, and only secondarily on the number of large magnitude earthquakes on a given day.

In conclusion, we furnished monitoring data on the activity rate of a Deep Seated Gravitational Slope Deformation in seismic context, we indicated two sectors of the investigated deformation that resulted more unstable and we proved that the combination of InSAR and GPS data is a useful monitoring system for earthquake-activated, slow-moving slope instabilities.

1.1. Introduction

Deep-seated Gravitational Slope Deformation (DGSD) is a generic term indicating rock-mass movements that encompass entire hillslopes or valley flanks (Dramis and Sorriso-Valvo, 1994; Agliardi et al., 2001) and that show diagnostic geomorphic features such as double ridges, trenches, and counterslopes (Goguel, 1978; Dramis and Sorriso-Valvo, 1994; Crosta and Zanchi, 2000; Crosta et al., 2013; Pánek and Klimeš, 2016). DGSDs are usually characterized by low deformation rates (few millimetres to 1-2 cm per year) and their activity is related to many factors, including seismic activity, erosional processes, rainfall, and post-glacial *debuttressing* (Radbruch-Hall, 1978; Bovis, 1982; Miller and Dunne, 1996; Crosta and Zanchi, 2000; Crosta et al., 2013). In spite of their low deformation rates, DGSDs can also experience acceleration and/or partial-collapse phases, which represent a significant hazard to people and infrastructures (Dramis and Sorriso-Valvo, 1994).

As highlighted by Pánek and Klimeš (2016), research on DGSDs has substantially increased in the past decade, with a focus on the application of monitoring techniques, the characterization of long- and short-term evolution, and the susceptibility to catastrophic collapses. However, there are still outstanding issues, including the need to better determine triggers and characterize changes in the movement rate of DGSDs. Before the first monitoring and dating studies, creep was considered to be the dominant mode of DGSD motion (Varnes et al., 1990). Although recent studies confirm that creep is the main mechanism (McCalpin and Irvine, 1995; McCalpin et al., 2011), in many cases data documented episodic and more rapid movements, especially in presence of active tectonic structures (McCalpin and Hart, 2003; Gutiérrez et al., 2008; Moro et al., 2012).

Some authors have recently investigated the correlation between seismic activity and DGSDs movement (Moro et al., 2007, 2011, 2012; Gori et al., 2014; Materazzi et al., 2015; Polcari et al., 2017). These authors documented coseismic displacements of DGSDs during magnitude (M_w)>5.0 earthquakes using Synthetic Aperture Radar Interferometry (InSAR) data and performing paleosismological analysis. All of these studies were conducted in the central Apennine, a seismically active mountain chain in Italy, where DGSDs and active faults are common. All authors reported evidences of episodic instantaneous DGSDs reactivation. In particular, in two cases, they linked these movements to the Colfiorito earthquake, which happened in Central Italy on September 26,′ 1997 (Moro et al., 2007; Materazzi et al., 2015) and, in one case, to the L'Aquila earthquake (Moro et al., 2011), which occurred on April 6, 2009, about 80km south of the previous one.

Moreover, after the M_w 6.0 Accumoli earthquake, occurred on August 24, 2016 about 40 km south of Colfiorito, Aringoli et al. (2016) documented DGSDs reactivation in the epicentral area.

The Accumoli earthquake was the first of a series of earthquakes that struck Central Italy between 2016 and 2017, severely damaging tens of villages and causing several fatalities. The seismic sequence includes an M_w 5.4 aftershock, one hour after the M_w 6.0 main shock, and tens of thousands smaller aftershocks, which pursued until the middle of September when the numbers of aftershocks decreased to about 100 earthquakes/day (Michele et al., 2016). Two months later, on October 26, M_w 5.9 and M_w 5.4 earthquakes occurred 20-30 km north of Accumoli, preceding the largest event of the sequence, an M_w 6.5 quake on October 30, 6 km north of Norcia (Fig. 1). All of the earthquakes had hypocenters at about 7-9 km depth along normal fault planes.

A series of earthquakes happened on January 18, 2017, 20 km south of the first event of the seismic sequence, damaging villages in the province of L'Aquila. The four strongest earthquakes of this series happened within four hours and had sources at depths of 9-10 km (Fig. 1).

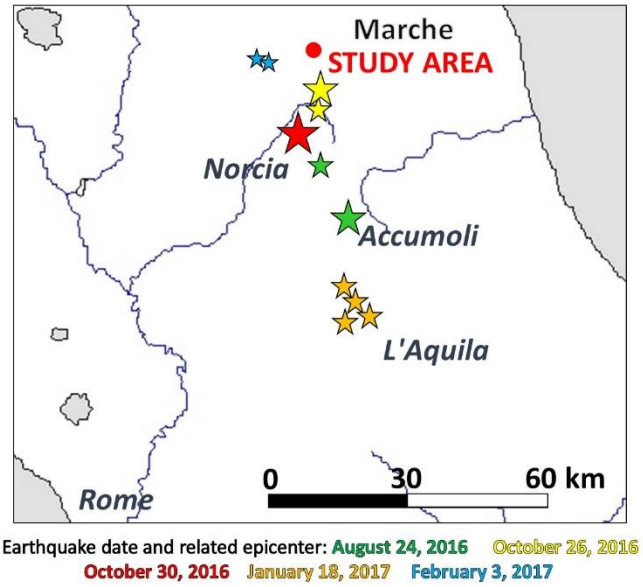

Fig. 1. Distribution of the epicentres of the largest earthquakes (M_w 5.0-to-6.5) of the 2016-2017 seismic sequence.

Considering the high seismicity of Central Apennines and that only 10% of DGSDs in this area can be explained by post-glacial *debuttressing* of formerly glaciated slopes (Aringoli et al., 2011), seismic activity must be considered an important trigger of deep slope movements in this region. Thus, investigations on the relation between historic earthquakes and DGSD motion is crucial for quantifying: i) the amount of any co-seismic DGSD displacements, ii) the minimum moment magnitudes and iii) the maximum distance of earthquakes capable to trigger movements.

We aim to contribute to the aforementioned issues by reporting the results of a monitoring program of a DGSD in Central Italy. We documented the pre-earthquakes evolution of the phenomenon and measured its seismically induced displacements during the 2016-2017 seismic sequence through GPS permanent stations and InSAR.

1.2. Geological and geomorphological context of the Fiastra DGSD

Our case study is located in Marche region, on the east side of Central Apennines. The investigated slope extends northward from the top of Mount Frascare, about 1300 m a.s.l., to the Fiastrone valley floor at about 600 m a.s.l. The Fiastra hydroelectric reservoir is located on the valley floor, and its dam lies at the foot of the investigated slope (Fig. 2).

The Jurassic and Cretaceous units of the marly-calcareous Umbro-Marchigiana stratigraphic succession (Lower Lias–Upper Eocene) underlie the study area (Calamita, 1994; Deiana et al., 2009). In detail, the following formations widely outcrop in the investigated slope: Maiolica Formation (Upper Tithonian – Lower Aptian), Marne a Fucoidi Formation (Lower Aptian – Upper Albian), Scaglia Bianca Formation (Upper Albian - Lower Turonian) and Scaglia Rossa Formation (Lower Turonian – Lutetian) (Aringoli et al., 2010) (Fig. 2). Maiolica has a total thickness up to hundreds of meters and is made of whitish limestone with concoidal fracturing and gray

or black chert (Deiana et al., 2009). The Marne a Fucoidi Formation consists of reddish, green and yellowish marls and clayey marls, and an overlying unit of whitish marly limestone; it is about 60 m thick (Deiana et al., 2009) and is the softest rock in the study area. Scaglia Bianca is a whitish limestone and marly limestone with black to reddish chert, 60-70 m thick (Deiana et al., 2009). Finally, the Scaglia Rossa Formation is composed of reddish limestone and marly limestone with red chert, and is several tens of meters thick (Deiana et al., 2009).

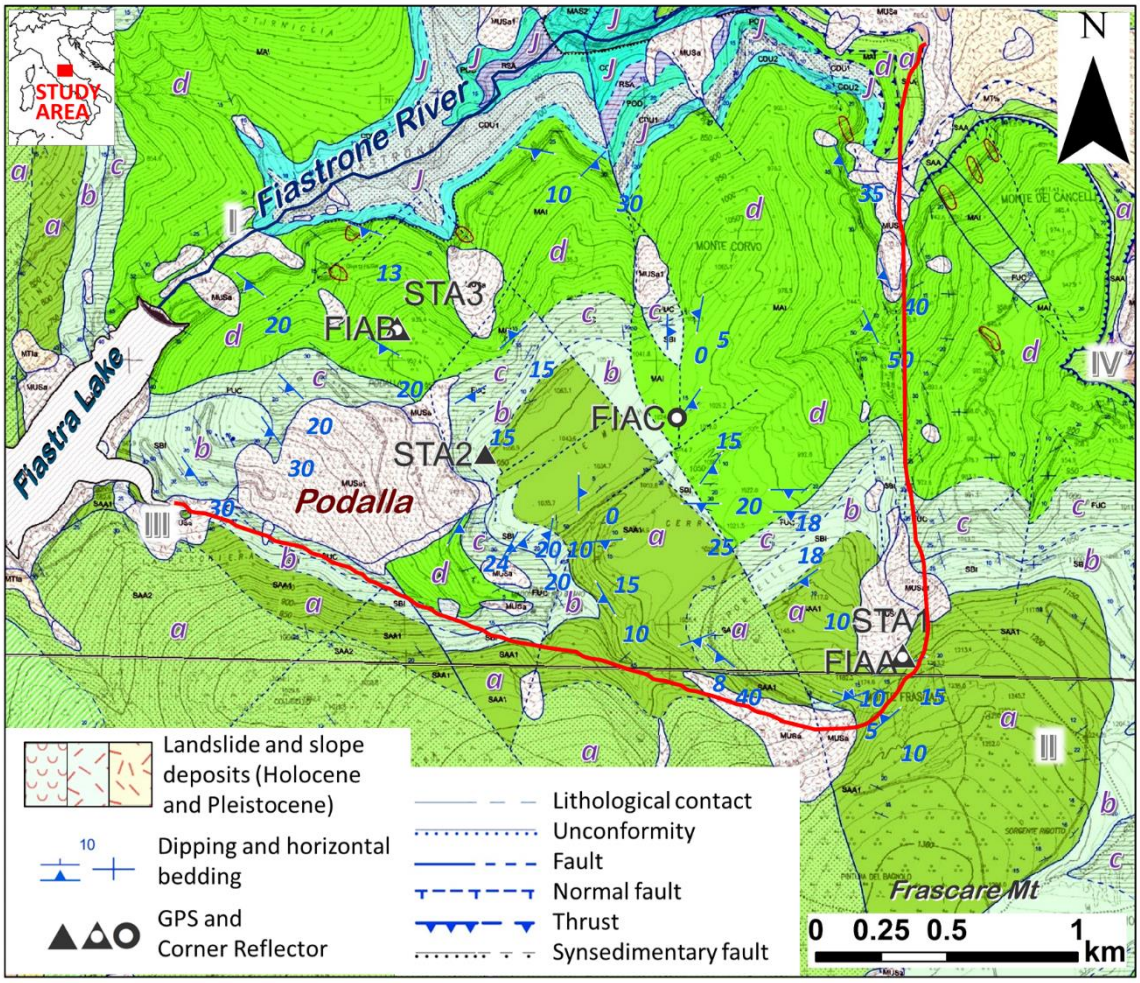

Fig. 2. Geological map of the study area (modified after Carta Geologica Regionale 1:10000 – Regione Marche, 2014): a) Scaglia Rossa Fm – several members; b) Scaglia Bianca Fm; c) Marne a Fucoidi Fm; d) Maiolica Fm; J) Jurassic formations. I-II and III-IV represent the traces of the geological sections. Red line indicates the area involved in the slope deformation.

The Umbro-Marchigiana succession underwent a compressive deformation during the Tortonian-Messinian, which generated the Apennine chain (Calamita, 1994). At that time, a sequence of thrust faults formed, producing shortening and tectonic overlaps. A shallow thrust plane that dips approximately 10° northwestward (Figs. 2 and 3) is present in the study area and the outcropping rocks are folded along an axial plane that strikes about N170°.

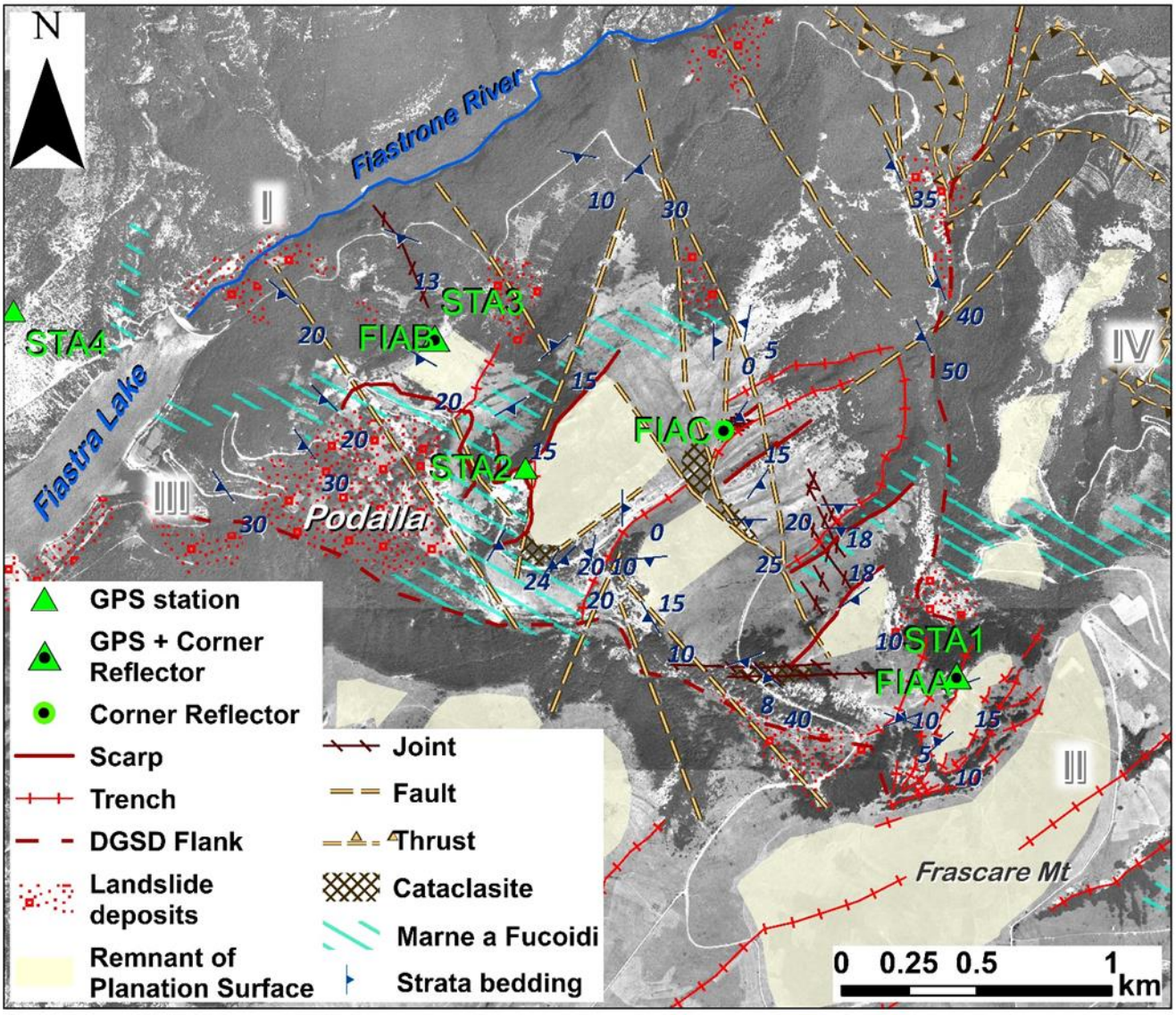

Fig. 3. Geomorphological map of the study area (modified after Tolomei et al., 2013). I-II and III-IV represent the traces of the geological sections.

Along almost the entire Apennine chain, the relief frequently results shaped by a gentle, rounded, high-elevation planation surface – the *Paleosuperficie* (Demangeot, 1965; Raffy, 1979). "Planation surface" is a descriptive term for a geographically plain surface resulting from erosion (Brown, 1969) and has not a genetic implication (Small, 1978). Coltorti & Pieruccini (2000) suggests that this surface was modelled very fast during the Lower Pliocene transgression.

Since the Late Pliocene/Lower Pleistocene, Central Apennines was the site of extensional tectonics related to a regional uplift that led to the opening of several intermontane basins and still goes on (Cavinato et al., 1994; Centamore et al., 2003). Related to this, the following systems of faults, with normal or transpressive kinematics, have been recognized in the study area (Figs. 2 and 3): Apenninic system (N150°–170°), anti-Apenninic system (N30°–50°) and N–S system (Aringoli et al., 2010; Tolomei et al., 2013).

The strong Pleistocene uplift induced the erosion of the planation surface that was incised by rivers and dissected by extensional tectonic structures. Minor erosional surfaces were modelled within the evolving drainage network and the remnants of the former *Paleosuperficie* were only locally preserved (Coltorti and Dramis, 1995).

In the study area, the Fiastrone River follows an important N30°–50° fault and formed a deep gorge at the toe of the investigated slope. Remnants of the Pleistocene planation surface are preserved in the study area, although they are displaced by numerous steps, counterslopes and meter-scale scarps related to the DGSD activity (Fig. 3). In detail, a system of trenches located over an area about 1 km long and 400 m wide, are present on the upper part of the slope. The trenches have a slightly curved shape, are roughly NE-SW oriented, up to 10 m deep, 20-30 m wide, and 800 m long (Figs. 3 and 4a, b). The largest ones are mostly vegetated and filled with debris (Fig. 4a, b), while the youngest ones are smaller, narrower and contain no debris or vegetation (Aringoli et al., 2010).

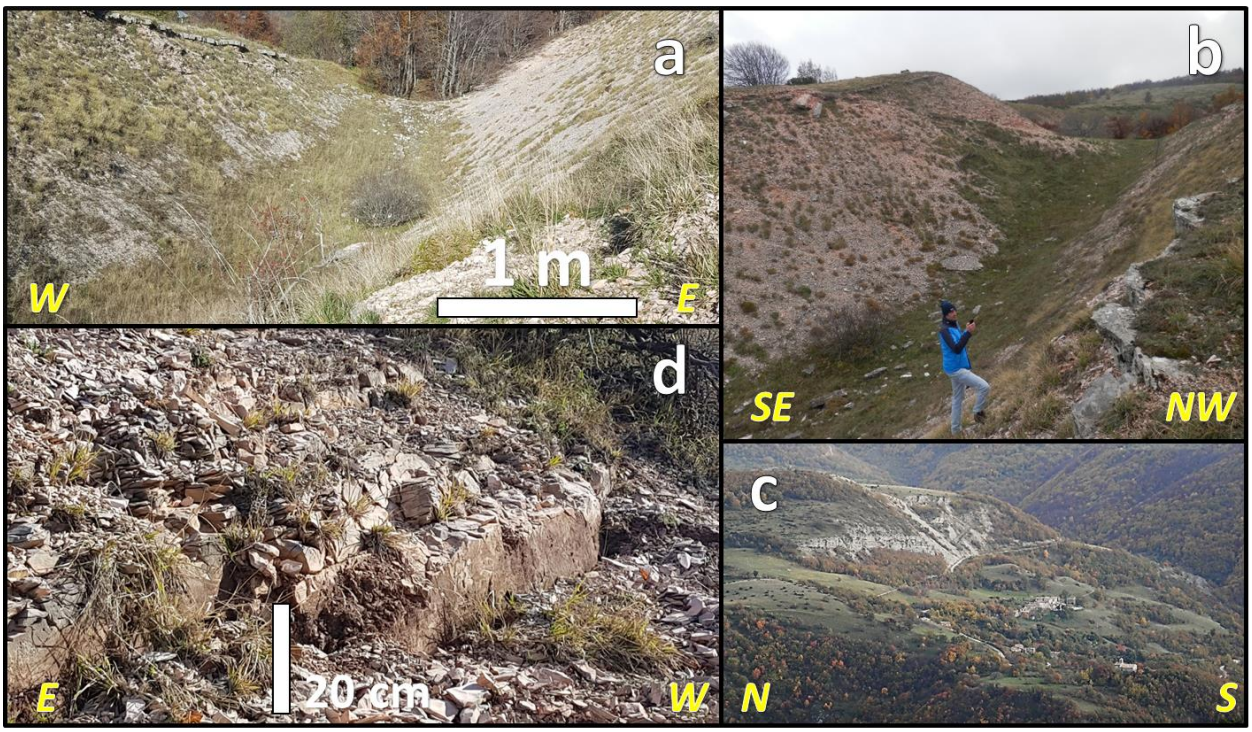

Fig. 4. a) and b) Upper trench of the Fiastra DGSD, close to STA1; c) Photo of Podalla landslide taken from STA4; d) New scarp formed in the upper trench, close to STA1, as consequence of the October 30, 2016 earthquake.

The presence of these features led to Tolomei et al. (2013) to state that the Fiastra DGSD (hereinafter FD) is a *sackung*, which is slowly moving towards the NNW along a gently dipping sliding plane and is upward bounded by curved trenches (Fig. 3). Previous studies (Aringoli et al., 2010; Tolomei et al., 2013) consider that the shallow thrust to the east (Figs. 2 and 3) is favourably oriented with respect to FD block movement and is a potential detachment surface. Moreover, Tolomei et al. (2013) observed an acceleration period in the FD InSAR time series that started at the end of September 1997. Therefore, they do not exclude that, as observed for other DSGSD in the area by Moro et al. (2007), FD was reactivated, at least locally and for a short period, by the M_w 5.7 and M_w 6.0 Colfiorito earthquakes, which occurred on September 26, 1997, 20km far away.

1.3. Material and methods

A multidisciplinary approach that combines field geomorphological survey, installation of permanent GPS stations, and InSAR elaborations was adopted for this study. The geomorphological survey was carried out to locate the best places to install four GPS stations and to update the existing cartography by mapping trenches and the remnants of the planation surface. Four corner reflectors were placed next to the GPS stations for satellite SAR acquisitions (Figs. 2 and 3).

The GPS network consists of four single-frequency stations (L1), using U-BLOX M8T chipsets, that transfer data in real time to the analysis centre at the Istituto Nazionale di Geofisica e Vulcanologia (INGV) in Rome (Italy) since October 2015. Three stations (STA1, STA2, and STA3) are distributed along the FD slope, close to the most significant geomorphological features of the DGSD; the fourth station (STA4) was placed on the opposite side of the valley and represents the reference point to which the measurements at the other three stations are referred (Fig. 3). STA1 and STA3 were previously equipped with double frequency receivers (Leica GX1230), named respectively FIAA and FIAB (Fig. 3) that operated from December 2014 until December 2016, thus acquiring one year of simultaneous observations. The single and double frequency stations were operated jointly to facilitate comparison of the results and for calibration purposes.

During the seismic sequence, the reference station (STA4) moved as consequence of ground shaking thus, we calculated the variation in length of the baseline between the uppermost (STA1) and the lowermost (STA3) stations and we used it as proxy to estimate the FD co-seismic deformation.

During the earthquakes on January 18, 2017, the GPS stations were buried by snow and stopped transmitting for one week. Moreover, STA2 suffered a transmission problem and only resumed operation following a site visit on March 24, 2017. Thus, we do not have the co-seismic displacements of the GPS points during the January 2017 earthquakes, and could only compare their positions before and after the seismic events.

The single frequency GPS data were processed using NDA-Lite software (Chersich and Curone, 2011). We show the time series and the map view of the three stations in the FD area in Figs. 9 and 10 respectively, as well as the variation in length of FIAA-FIAB/STA1-STA3 baseline (Figs. 11 and 13). The double frequency GPS data were processed with BERNESE software (Beutler et al., 2007) using a standard analysis procedure (Devoti et al., 2011). We plotted the resulting FIAA-FIAB/STA1-STA3 baseline time series with those of potential triggering factors (i.e. temperature, rainfall, and earthquakes) to determine which of the triggering factors is more important (Figs. 11 and 13). Meteorological data have been taken from the station at Pintura, about 10 km south of the study area.

The InSAR analysis have been performed with X-band Cosmo-SkyMed (CSK) and C-band Sentinel-1 data, which cover both valley walls of Fiastrone River and Fiastra Lake. In particular, CSK dataset used in this work consists of 29 SAR images acquired from February 2011 to October 2015. They were acquired along descending orbit with an incidence angle of ~34° and an azimuth angle of ~-169°. The data were multi-looked by factors 5x5 to reduce the speckle noise thus obtaining a pixel size of about 10m along both range and azimuth directions. We applied the InSAR technique estimating 195 interferograms by setting the thresholds for the maximum perpendicular and temporal baselines to 800m and 500days, respectively. The topographic phase component was removed by the 10 m TINITALY Digital Elevation Model (DEM). Then, we exploited the multi-baseline/multi-temporal Interferometric Point Target Analysis approach in the framework of the GAMMA software packages (Werner et al., 2003) for retrieving the point time series of the observed scene.

Concerning the Sentinel-1 SAR data, the results have been already presented in Polcari et al. (2017). The InSAR analysis was performed by means of two pairs of descending data acquired on August 21st and 27th 2016, and on October 25th and 31st 2016. The two retrieved interferograms were filtered by Goldstein filtering (Goldstein and Werner, 1998) and unwrapped by using the Minimum Cost Flow phase unwrapping algorithm (Costantini, 1998). The 30 m SRTM DEM was exploited to remove the topographic component.

1.4. Results

Based on field survey, we mapped the remnants of the planation surface throughout the study area. It is generally linear and has a low gradient. Its shape has been probably influenced by the gently dip of the strata (<20°) although the latter changes according to the presence of tectonic features as the main normal faults and the thrust plane (Fig. 3). Scarps and trenches related to slope instabilities abruptly interrupt the spatial continuity of the planation surface even outside the FD area, indicating that several portions of the southern flank of Fiastrone valley are affected by gravitational slope deformation (Fig. 3).

In detail, the presence of trenches at the summit, as well as counterslopes, many other trenches and scarps in the middle part of the slope (Figs. 3 and 5) led to concur with Tolomei et al. (2013) that FD is a *sackung* type deformation.

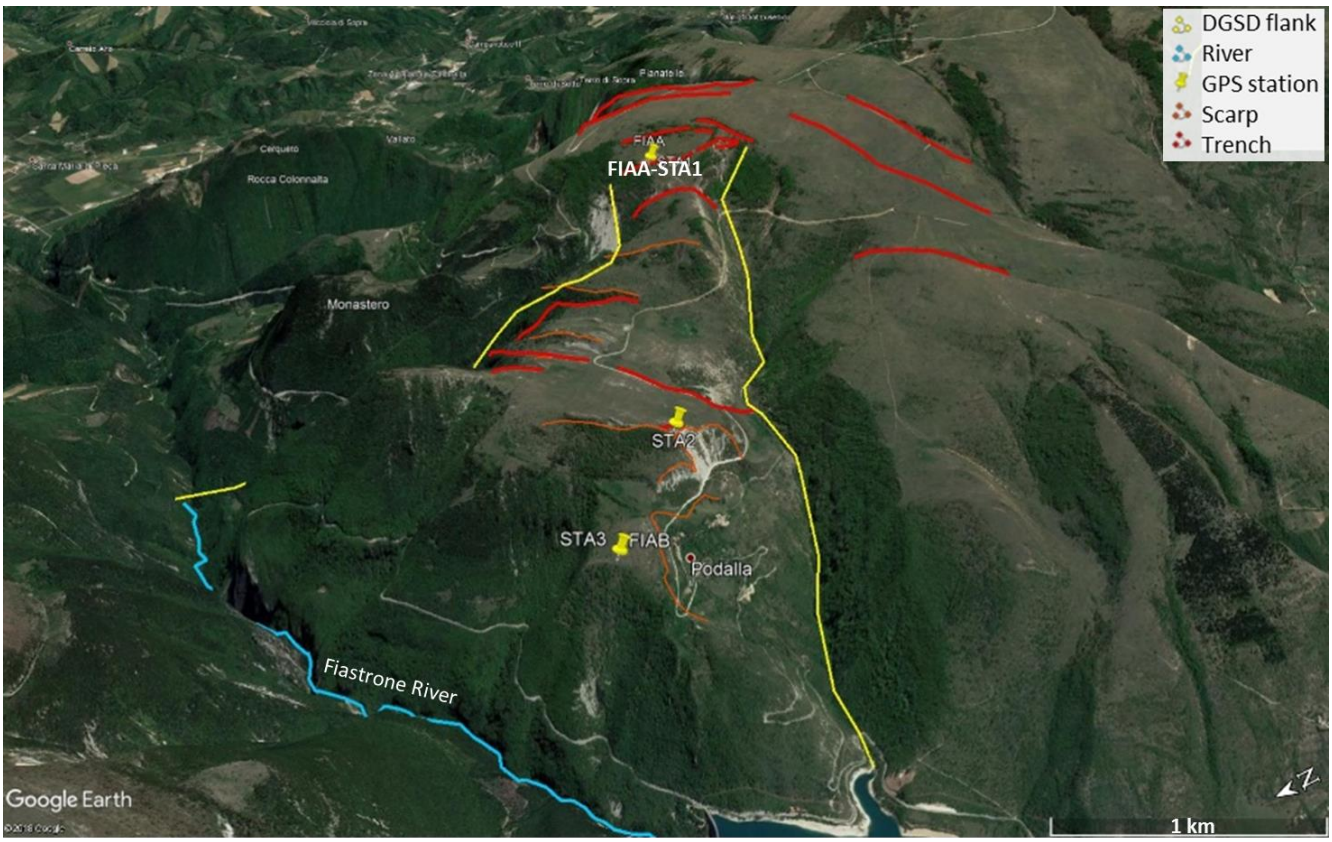

Fig. 5. Google Earth image including the main features of FD.

Moreover, by analysing the stereonet of the main tectonic and geomorphological features mapped during the field survey, it resulted that many scarps are parallel to fault directions, as like the right flank of FD, testifying a structural influence on the FD shape. On the other hand, the left flank of FD appears to be almost perpendicular to many fault directions, as like to some scarps and trenches, indicating that its formation may be the direct consequence of the FD movement and has not to be necessarily related to pre-existing planes (Fig.6). The orientation of all the geomorphic features, and their distribution (Fig. 5), allows to confirm that the expected direction of movement of FD is NNW.

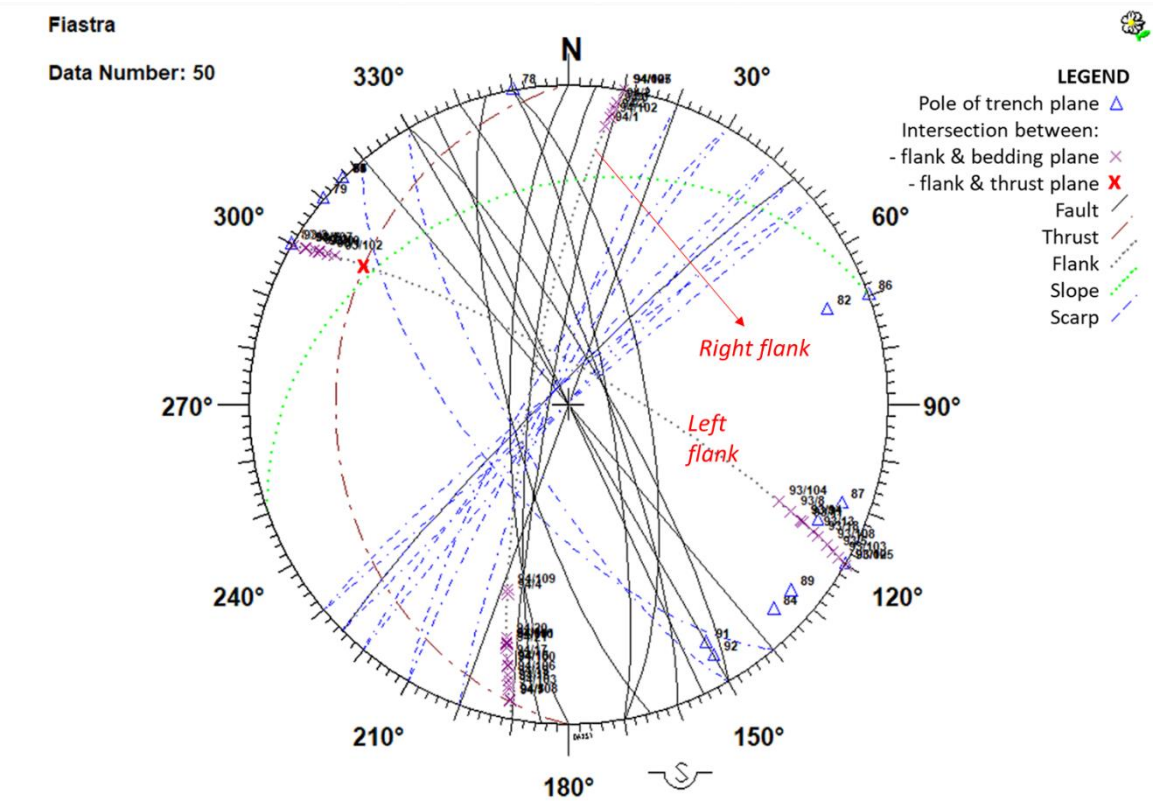

Fig. 6. Sterenoet has been computed trough Daisy 3 software.

If we consider the intersections between the FD flanks and both the bedding and the thrust plane, we observe that the intersections occur at lower angles than the slope angle, indicating the presence of potential sliding surfaces favourably oriented with respect to the slope. In particular, the intersection with the thrust plane is closer than the bedding to the slope projection (Fig. 6). This means that the bedding planes would require lower friction angle than the thrust plane in order to be kinetically free. This allows to state that strata bedding is not likely to be a preferential predisposing factor for the FD sliding and this can be seen as the consequence of the general low dipping of the strata and their highly variable direction.

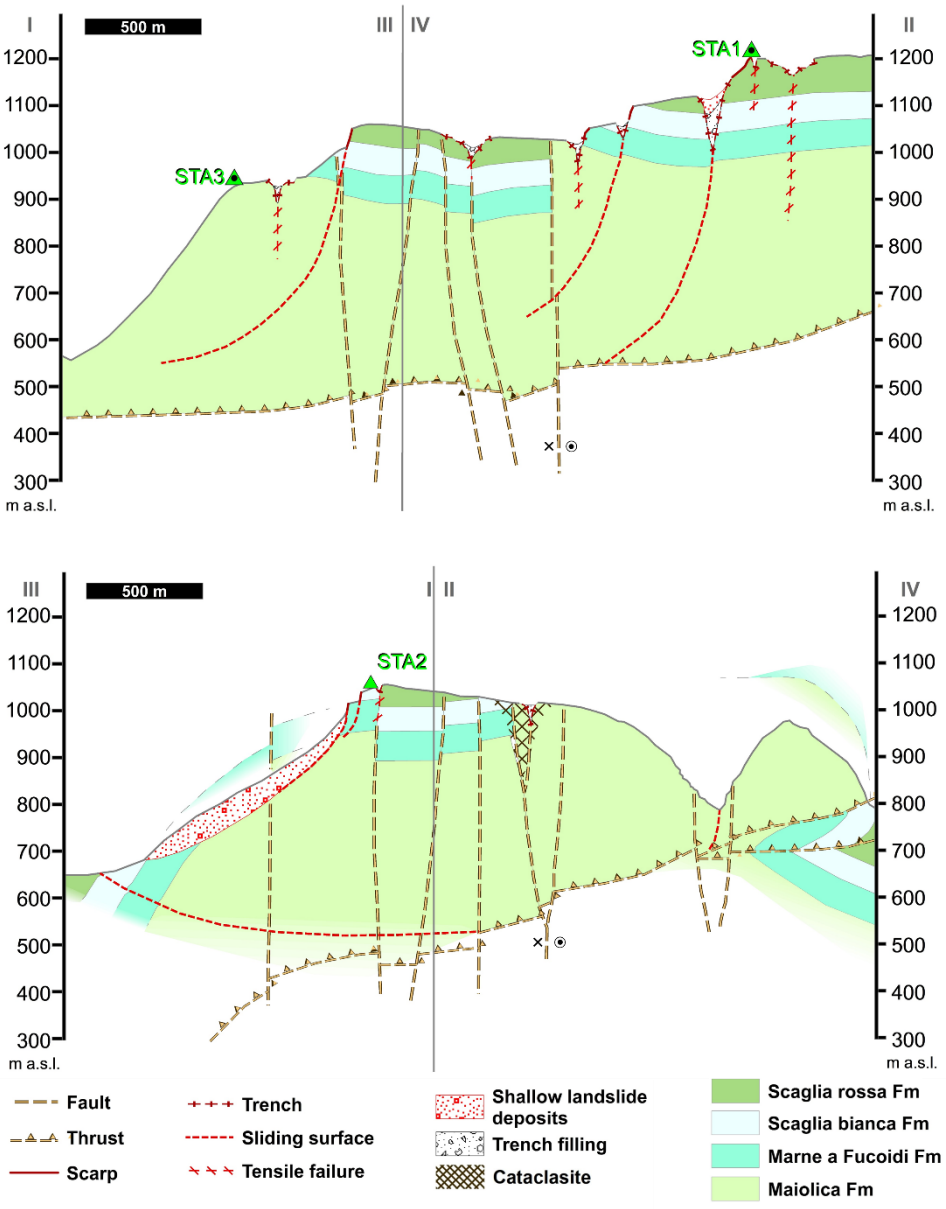

Fig. 7. I-II and III-IV geological sections. Vertical exaggeration is 2:1.

The geological sections (Fig. 7) show the general low dipping of the strata and its variability, supporting the inference that the bedding is not among the primary causes of FD. Fig 7 also shows that many scarps and trenches formed in correspondence of pre-existing tectonic features, although some sliding surfaces are probably of new generation. These surfaces have high-angle dipping that probably decreases with depth where they may be connected to the thrust plane. This latter can represent the low-angle basal portion of the sliding surfaces, as proposed in the past (Aringoli et al., 2010; Tolomei et al., 2013). Nevertheless, as shown in the section III-IV, when the thrust goes deeper, increasing its dipping, we cannot exclude that a new low-angle surface is exploited for sliding.

However, the proposed schemes should be validated with underground data to be completely reliable. At this stage, they only represent a hypothesis to describe the internal structure of FD.

To conclude, on the left flank of FD, we mapped the main scarp of the Podalla landslide, a minor and shallower failure (Figs. 3, 4c, 7 and 8) that shows signs of possible reactivation and was already studied by Aringoli et al. (2010). In this site, strata bedding is parallel to the slope, Marne a Fucoidi Fm widely outcrops and the lower part of the slope is covered by landslide deposits consisting of decimetric to metric calcareous blocks (Figs. 2, 3 and 7). Moreover, a rockfall source area is present upslope of the main scarp of Podalla landslide and shows features of an incipient enlargement, such as fractures. Here STA2 was placed (Fig. 8). Based on the field survey and the geological section (Fig. 7), we conclude that the Podalla landslide may be considered as a rockslide probably induced by the dipping of the strata and the presence of Marne a Fucoidi Fm, as previously stated by Aringoli et al. (2010). This instability may also induce the uppermost rockfall causing a general retreat of the slope parallel to the left flank of FD.

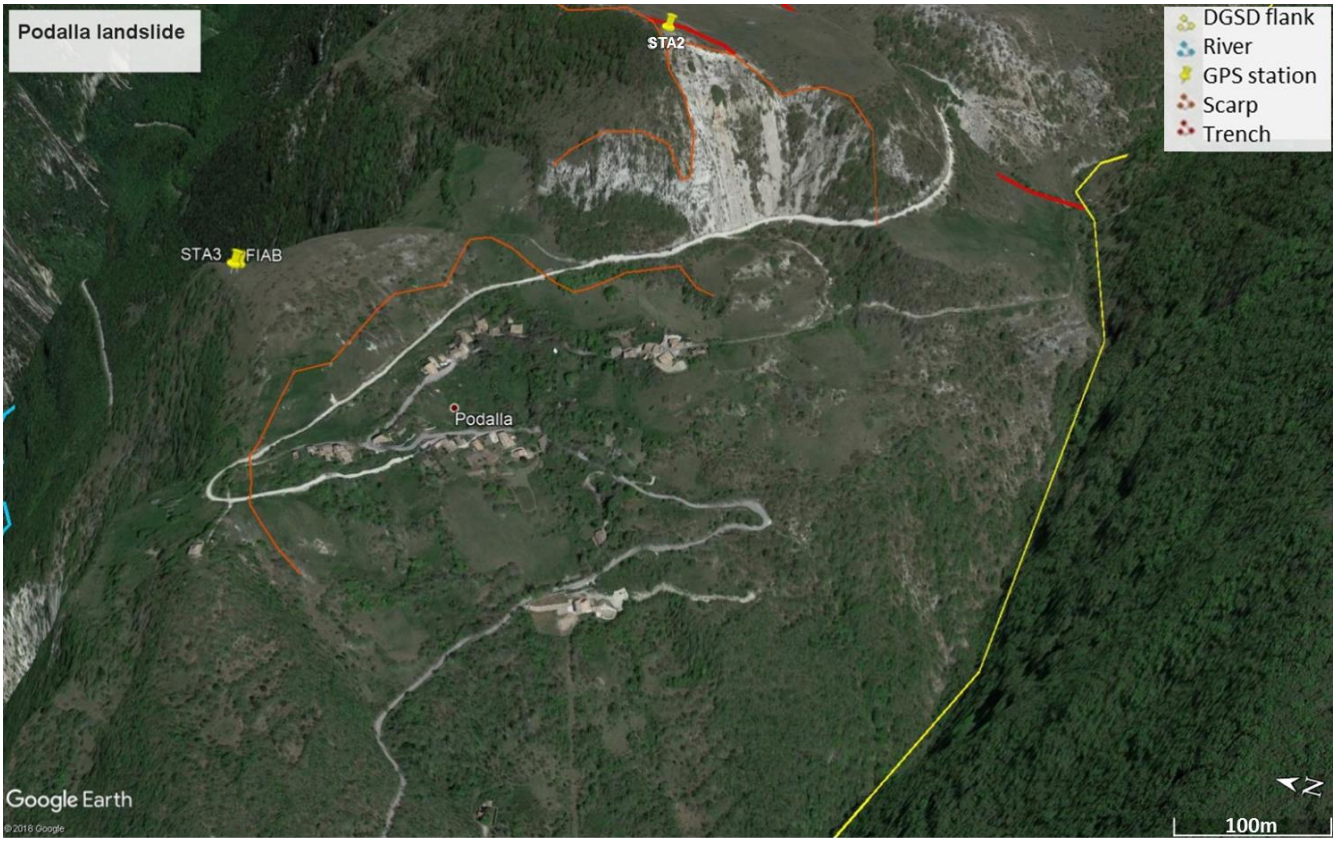

Fig. 8. Google Earth image including the main features of Podalla landslide.

The three GPS stations recorded significant movements, both horizontal and vertical, during the largest seismic events (M_w> 5.0) of the 2016-2017 seismic sequence in Central Italy (Fig. 9). However, at the time of the first

two earthquakes, only STA1 experienced significant changes in its position, above the slow background rate, with about 20-30 mm of movement toward the NNW and about 30 mm downward (Figs. 9 and 10).

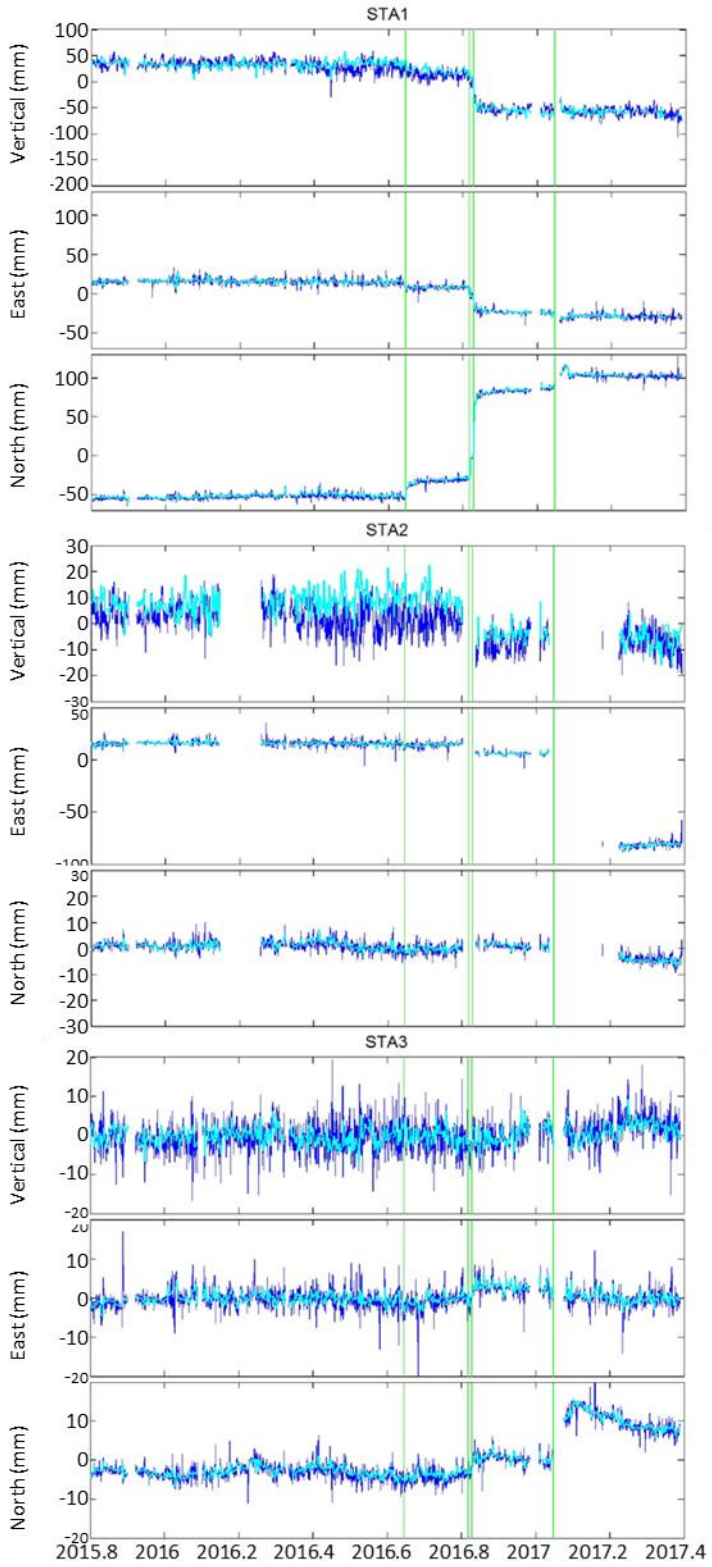

Fig. 9. Movement of each GPS station along vertical, east-west, and north-south directions from October 2015 to March 2017; vertical green lines indicate the occurrence of the largest earthquakes (M_w 5.0-to-6.5).

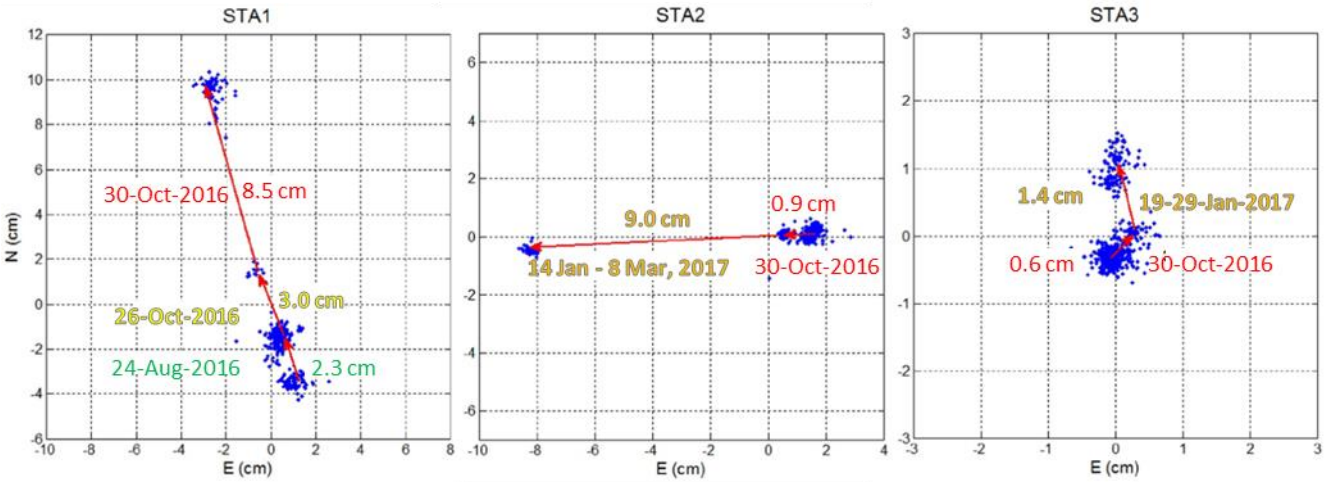

Fig. 10. Horizontal displacement of each GPS station during the main earthquakes: blue points indicate the hourly estimates of the position of the station, red arrows indicate the movement vector of the GPS station along the horizontal plane at the time of the earthquakes, the occurrence of the seismic event and the correspondent displacement is written close to the arrows. When technical problems occurred during the earthquake, the correspondent displacement refers to longer periods.

Later, during the October 30, 2016 earthquake, which was the strongest of the whole sequence (M_w 6.5), all three GPS stations recorded appreciable movements (Figs. 9 and 10). STA1 moved about 85 mm toward the NNW (Fig. 10) and 40 mm downward (Fig. 9), STA2 moved 9 mm westward (Fig. 10) and about 20 mm downward (Fig. 9), and STA3 moved 6 mm toward the NE (Fig. 10). The ground shaking also produced some field evidences generating a new, centimetric, scarp in the calcareous bedrock cropping out near to STA1 (Fig. 4d).

Finally, although we could not directly measure the co-seismic displacement stemming from the M_w>5.0 earthquakes on January 18, 2017, STA1 and STA3 showed about 15 mm movement toward NNW (Figs. 9 and 10) and STA2 recorded a westward displacement of 90 mm after we restored the antenna some weeks later (Fig. 10). This rather high displacement may be affected by an unknown deformation caused by the snow cover or bad weather conditions. Nevertheless, as mentioned above, STA2 is upslope of the main scarp of the Podalla landslide (Fig. 8) and the westward movements experienced during the earthquakes are consistent with potential direction of movement of the instability.

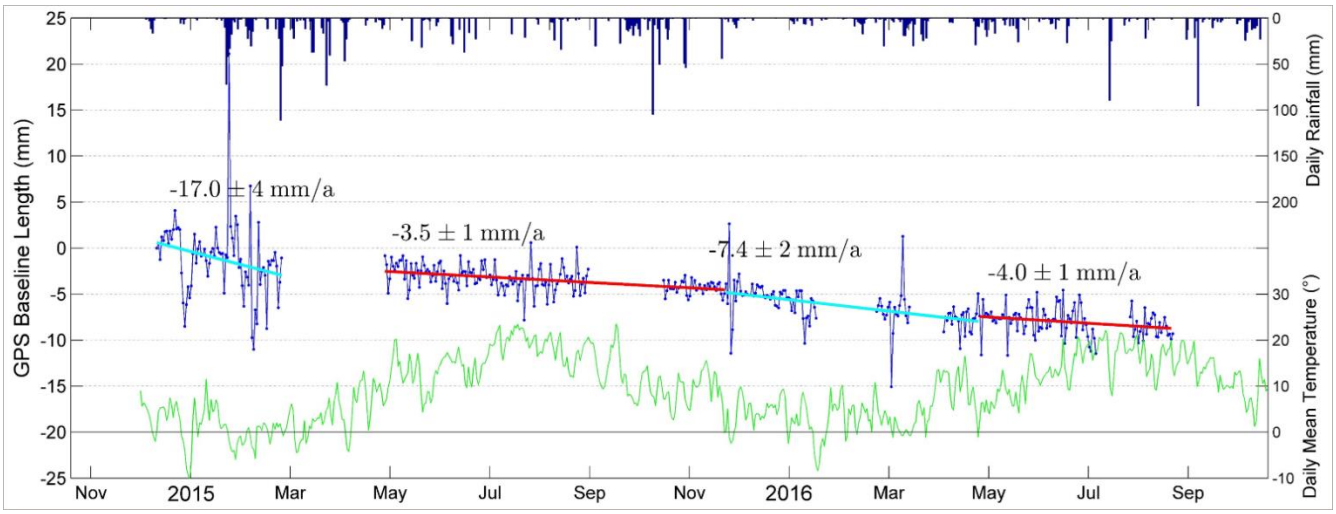

Fig. 11. Variation in the length of STA1-STA3/FIAA-FIAB from December 2015 to August 2016, measured with double frequency antennae and plotted with daily mean temperature (green line) and daily rainfall (blue histogram).

Figures 11 and 13 show the daily estimates of the length of the FIAA-FIAB baseline (Cartesian distance) before and during the earthquakes. Before the seismic sequence, from December 2014 to August 2016, the average baseline shortening rate was about 5mm/y, as detected by both single and double frequency GPS (green and blue dotted lines in Fig. 13). We detected increasing rates during cold periods (light blue in Fig. 11) and reduced rates in summer (red line in Fig. 11). In particular, we observed shortenings of 17 and 7.4 mm/y in winter and 3.5 and 4 mm/y during warmer periods (Fig. 11). This shortening does not seem to be related to rainfall (blue histogram in the upper part of the Fig. 11). In general, the shortening of the baseline can be attributed to different movement rates between STA1 and STA3. In detail, the uppermost station (STA1) is most likely the moving site that causes the progressive decreasing of the distance between the two stations observed in Fig. 11.

In winter, temperatures are frequently below 0°C, thus we might interpret the higher shortening rates as due to ground volume changes that are probably related to shallow processes due to freeze-thaw cycles. The lower rates (<5mm/y) movement in warm periods can be considered representative of the DGSD activity, because no external processes appear to be involved.

Therefore, in absence of other factors, the incision of Fiastrone River, whose valley is very narrow and deep, can be considered an important underlying cause of the low, apparently constant, deformation rate of FD. Although this has been as observed in numerous similar cases in Central Apennines (Galadini, 2006; Aringoli et al., 2010), to calculate the incision rate of Fiastrone river would be required to confirm this consideration.

The notable fluctuations in baseline length during cold periods, which occasionally shortens or lengthens the baseline length by several millimetres but does not induce permanent displacements, seem to coincide with freezing temperatures <0°C (see green line in Fig. 11). At this stage of our research, we could argue that ice or snow cover on the GPS antenna may have caused an apparent shift of the antenna phase centre (the ideal point where the GPS signal is detected), producing the observed shifts in position.

The InSAR elaborations of COSMO-SKYMED images from 2011 to 2015, confirm that, in the study area, the ground deformation, as measured along the line of sight, is very small (Fig. 12a) and that it did not experience significant oscillations thought time (Fig. 12b).

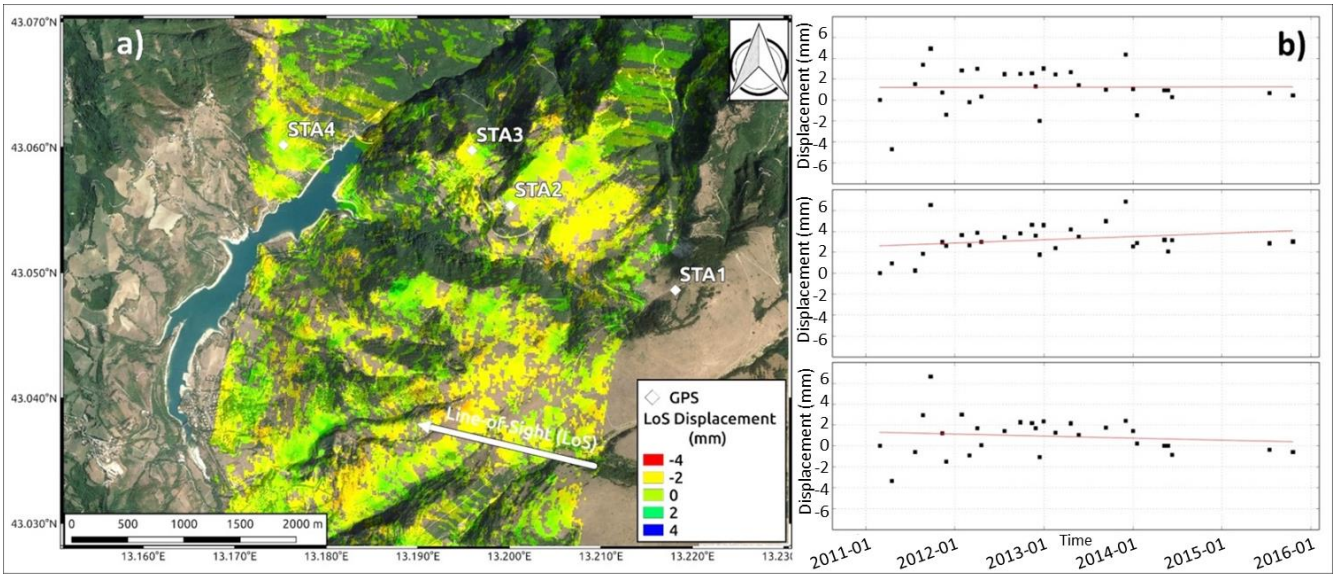

Fig. 12. a) Ground deformation in the study area detected by InSAR of COSMO-SKYMED satellite images during the period February 2011 - October 2015; b) Time series of ground deformation in the proximity of STA3.

After the seismic sequence started in Central Italy, the STA3-STA1 baseline experienced one-order-of-magnitude higher instantaneous episodes of shortening during the strongest earthquakes (coloured stars in Fig. 13 – number inside indicates the magnitude). The baseline shortened in a NNW direction, almost perpendicular to the main trenches of FD and in line with the direction of movement previously inferred. The shortening is mainly due to valleyward movement of STA1, since STA3 experienced small displacements (Fig. 9). The baseline shortened by about 10, 25, and 55 mm during, respectively, the August 24, October 26, and October 30, 2016, seismic events (Fig. 13). STA 1 and STA 3 experienced the same amount of displacement only during the earthquakes of January 2017 (Fig. 9) thus they did not vary their distance at this time (Fig. 13).

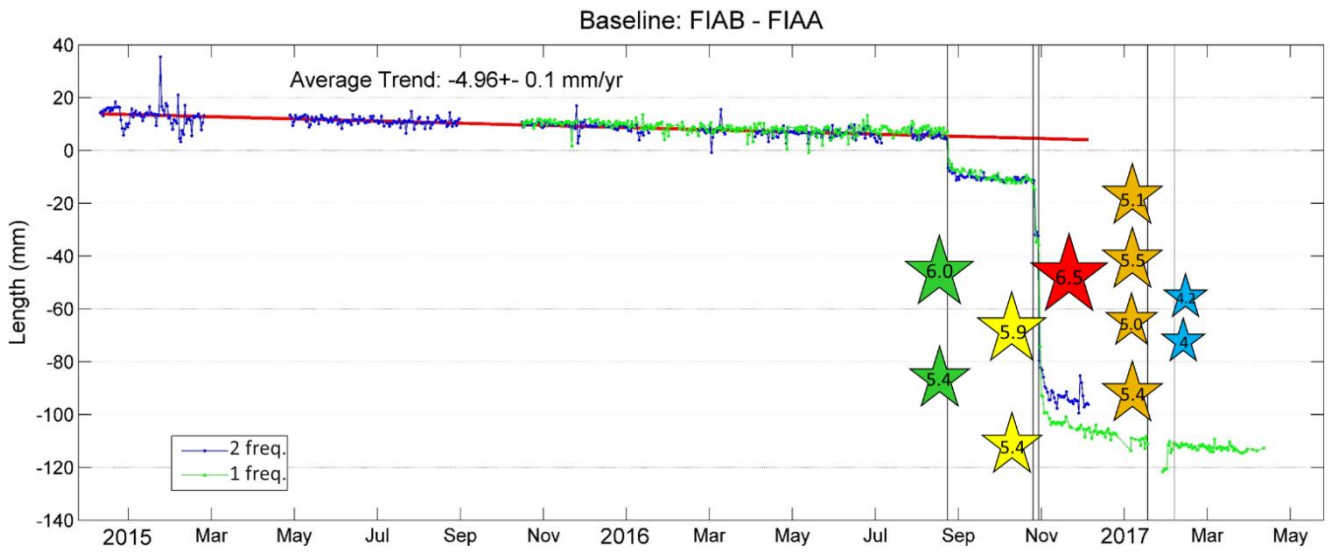

Fig. 13. Variations in the length of STA1-STA3/FIAA-FIAB from December 2015 to April 2017, measured by single and double frequency antennae and plotted with the main earthquakes of the seismic sequence (coloured stars – number inside is the magnitude).

We observed that the stronger the earthquake, the greater the amount of shortening of the baseline, although the relationship is non-linear. In detail, an exponential model best describes the fit with our data (Fig. 14a). The earthquakes in February 2017, although very close to our study area (about 15 km), were not large enough to cause appreciable movements of FD. Nevertheless, the distances from the epicentres played a significant role on the baseline shortening. The events of August 24 and October 26, 2016 (Fig. 14b) had nearly the same magnitudes, but they caused significantly different displacements. The first of the two was considerably farther from FD than the second and produced lesser displacements (Fig. 14b). Distance also seems to conceal the potential effect of the number of M_w>5.0 earthquakes that happened during a single day. In January 2017, four M_w>5.0 earthquakes happened within one day, yet only a few millimetres of change in the baseline length was observed because they were very far from FD (>60 km) (Fig. 14b).

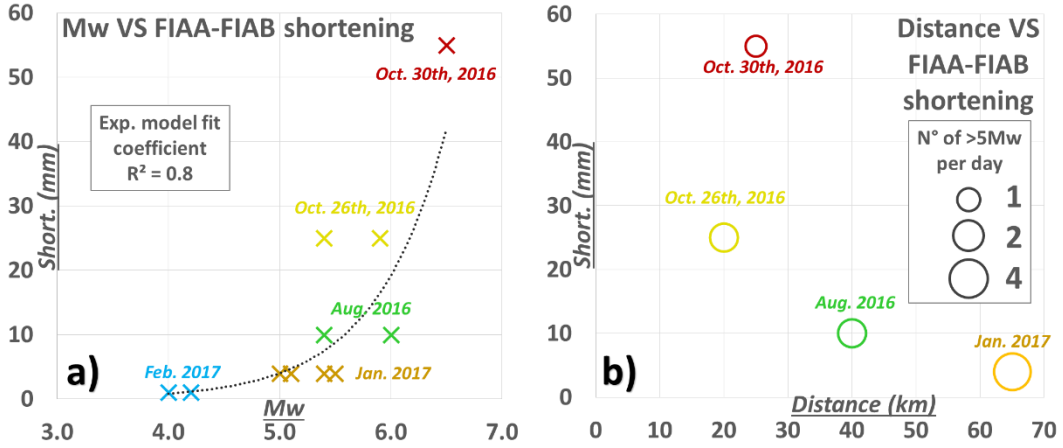

Fig. 14. a) FIAA-FIAB baseline shortening plotted against the magnitude of the main earthquakes of the sequence. The stronger the earthquake, the larger the shortening, in accordance with a non-linear correlation. In detail, the exponential model best fits our data. b) FIAA-FIAB baseline shortening plotted against epicentral distance of the main earthquakes of the sequence. Size of circles represents the number of strong earthquakes (M_w>5) on the same day.

InSAR analysis of Sentinel-1 images, presented in Polcari et al., 2017, allowed to compare with GPS measurements and to investigate the ground deformation in those areas where GPS stations are not present. InSAR data confirmed that, in proximity of STA1, the ground did not move the same that in STA3 at the time of Accumoli (Fig. 15A) and Norcia (Fig. 15B) earthquakes although values of deformation are not the same between InSAR and GPS (Tab.1). In general, with respect to GPS measurements, InSAR underestimates STA1 displacement (it is not detected during the first event, Fig. 15A) and overestimates the movements of STA3, whereas values of STA2 are in accordance (Tab. 1).

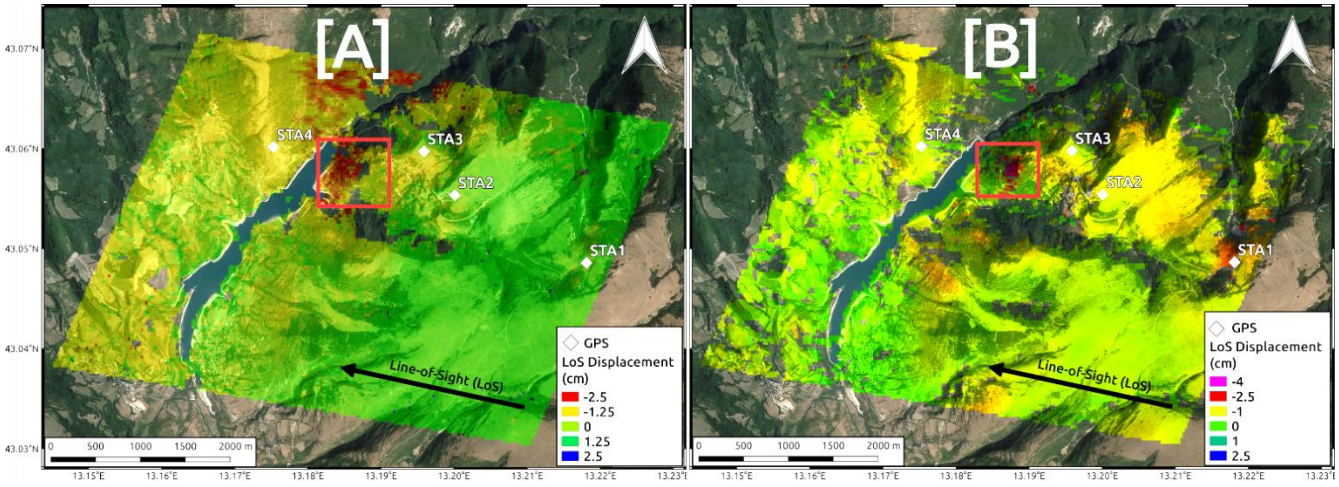

Fig. 15. Ground deformation in the study area detected by InSAR of Sentinel-1 images during the A) Accumoli (August 24, 2016) and B) Norcia (October 30, 2016) earthquakes (modified after Polcari et al., 2017).

Moreover, a cumulative displacement up to 60 mm along the radar line of sight was measured on the lower part of the slope, downslope of STA3 (red square in Fig. 15), as consequence of Accumoli (Fig. 15A) and Norcia (Fig. 15B) earthquakes. This can indicate the presence of a shallow process in this sector of the FD, as a rockslide, which moves with higher rate than the deep deformation affecting the whole slope. Furthermore, especially during the first event, a large area on the opposite side of the valley experienced a significant displacement of about 20 mm (Fig. 15A). This latter point implies a possible movement of the GPS reference station that has to be further investigated and, if the deformation will persist, it should become visible in the STA4 GPS time series as well.

	Accumoli (August 24th, 2016)		Norcia (October 30th, 2016)	
Point	**GPS (cm)**	**InSAR (cm)**	**GPS (cm)**	**InSAR (cm)**
STA1	-1.2 ± 0.7	0.2 ± 0.5	-7.6 ± 0.6	-3.1 ± 0.5
STA2	-0.02 ± 0.5	-0.04 ± 0.5	1.6 ± 0.4	-1.0 ± 0.5
STA3	0.01 ± 0.3	-0.15 ± 0.5	-0.02 ± 0.3	-0.9 ± 0.5

Tab. 1. Comparison of Sentinel-1 InSAR and GPS measurements, projected along the satellite line of sight.

The partial discordance between InSAR and GPS can be due to different reasons. First, the error associated to the measures has to be considered (Tab. 1). This is of about 0.5 cm in the calculation of ground deformation and 1-1.5 mm/y in the calculation of mean ground velocity for InSAR technique. Moreover, we cannot exclude the potential influence of the possible movement of the reference station on the GPS measures. Finally, the proximity of Fiastra Lake, which has a high level of water vapour especially in the summer season, could give rise to an atmospheric effect that might influence InSAR data (Polcari et al., 2017).

Thus, considering all these aspects, the accordance between the two techniques is generally good.

1.5. Conclusions

By integrating the information provided by both InSAR and GPS acquisitions, we can conclude that the Fiastra DGSD (FD) experienced significant step-like accelerations during the seismic sequence of Central Italy in 2016 and 2017. In detail, the normal average activity rate in absence of M_w>5.0 earthquakes is very slow, linear and probably associated with creep-type motion. This rate does not appear to be homogeneous in every sector of the DSGD but is generally lower than 3 mm/y. In detail, the area of the uppermost trenches, i.e. in the vicinity of STA1, likely moves faster than the lowest sector of the DSGD, where STA3 is placed.

Despite some winter acceleration that we attribute to shallow processes due to freeze-thaw cycles, no correlation between rainfall and the normal creep activity rate of the DSGD was observed. Therefore, although the influence of rainfall and snowmelt cannot be completely ruled out, we consider that the erosion of the toe of the slope by Fiastrone River may represent an important causative factor for the normal movement rate of the deformation. We conclude that the mass movement (a *sackung* type) exploits the high-angle pre-existing tectonic discontinuities, and perhaps a basal low-gradient thrust fault. The presence of other DGSD-like geomorphological features elsewhere on the slope confirms the predisposition of the whole valley to this type of phenomenon.

On the other hand, the step-like accelerations triggered by earthquakes, are one to ten times higher than the average normal activity rate of the Fiastra DGSD. In detail, the movement mainly depended on the magnitude of the earthquake and the distance from the epicenter, and only secondarily on the number of big earthquakes on a given day. We measured about 60 mm as the maximum instantaneous deformation, which occurred during an M_w 6.5 earthquake about 25 km far from the study area. Earthquakes smaller than M_w5.0 or farther than 70 km from the study area did not produce significant movements of the Fiastra DGSD.

Moreover, InSAR detected significant movements of a large area in the lower part of the Fiastra DGSD during the August 24, 2016 and October 30, 2016 earthquakes. In addition, along the southern flank of the DGSD, the GPS station placed in the Podalla landslide area, which shows field evidences of recent past activity, experienced 1 to 10 cm westward displacement during the October 30, 2016 and January 18, 2017 earthquakes. Therefore, we conclude that these two sectors of the Fiastra DGSD currently represent the most hazardous sites in the study area because the slope at those sites resulted particularly unstable and moving faster.

Regarding the methods adopted in this work, we found a generally good accordance between single and double frequency GPS receivers, in spite a gap during the earthquakes sequence. Thus, we consider that the low-cost GPS system that we tested is reliable and can be used in similar studies although the sensitivity of the instrument to bad weather conditions suggests particular care in arranging reliable antenna supports and placing. A characteristic of GPS systems is that they furnish only point data, thus areal patterns cannot be directly measured, but rather must be inferred.

In conclusion, we consider that the combination of InSAR and GPS data is a useful monitoring system for earthquake-activated, slow-moving landslides. In particular, InSAR techniques provide areal data that can be useful to extend the GPS point data over large areas. Moreover, SAR measurements are not subject to the weather limitations of GPS. On the other hand, we have to consider that, at present, SAR can only make measurement along the satellite line of sight and thus is likely less accurate that GPS.

1.6. Acknowledgements

The authors want to thank the editors and reviewers for the constructive feedbacks during the revision process. Authors do also thank the European Space Agency (ESA) and the Italian Space Agency (ASI) for providing Sentinel-1 and CosmoSkyMed SAR data, respectively.

1.7. References

Agliardi, F., Crosta, G., & Zanchi, A. (2001). Structural constraints on deep-seated slope deformation kinematics. Engineering Geology, 59(1), 83-102.

Aringoli, D., Farabollini, P., Giacopetti, M., Materazzi, M., Paggi, S., Pambianchi, G., Pierantoni, P.P., Pistolesi, E., Pitts, A., & Tondi, E. (2016). The August 24th 2016 Accumoli earthquake: surface faulting and Deep-Seated Gravitational Slope Deformation (DSGSD) in the Monte Vettore area. Annals of Geophysics, 59.

Aringoli, D., Gentili, B., Materazzi, M., & Pambianchi, G. (2010). Mass movements in the Adriatic Central Italy: activation and evolutive control factors. Landslides: causes, types and effects. Nova Science Publishers Inc., New York, 1-71.

Aringoli, D., Gentili, B., Materazzi, M., Pambianchi, G., & Sciarra, N. (2013). DSGSDs induced by post-glacial decompression in central Apennine (Italy). In Landslide Science and Practice, 417-423. Springer Berlin Heidelberg.

Beutler, G., Bock, H., Dach, R., Fridez, P., Gäde, A., Hugentobler, U.P., Jäggi, A., Meindl, M., Mervart, L., Prange, L., Schär, S., Springer, T., Urschl, C., Walser, P. (2007). Bernese GPS Software Version 5.0. Bern: Astronomical Institute, University of Bern.

Bovis, M.J. (1982). Uphill-facing (antislope) scarps in the Coast Mountains, southwest British Columbia. Geological Society of America Bulletin, 93(8), 804-812.

Calamita, F., Cello, G., Deiana, G., & Paltrinieri, W. (1994). Structural styles, chronology rates of deformation, and time-space relationships in the Umbria-Marche thrust system (central Apennines, Italy). Tectonics, 13(4), 873-881.

Carta Geologica Regionale 1:10000 – Regione Marche (2014) Regione Marche – P. F. Urbanistica, Paesaggio e Informazioni Territoriali. http://www.ambiente.marche.it/Territorio/Cartografiaeinformazioniterritoriali/Archiviocartograficoeinformazioniterritoriali/Cartografie/CARTAGEOLOGICAREGIONALE110000.aspx

Cavinato, G.P., Cosentino, D., De Rita, D., Funiciello, R., & Parotto, M. (1994). Tectonic-sedimentary evolution of intrapenninic basins and correlation with the volcano-tectonic activity in Central Italy. Memorie Descrittive della Carta Geologica d'Italia, 49, 63-76.

Centamore, E., Dramis, F., Fubelli, G., Molin, P., & Nisio, S. (2003). Elements to correlate the marine and continental sedimentary successions lying on the Latium and Abruzzo margins of the Apennines. Il Quaternario, 16, 77-87.

Coltorti, M., & Dramis, F. (1995). The chronology of upper Pleistocene stratified slope-waste deposits in central Italy. Permafrost and Periglacial Processes, 6(3), 235-242.

Coltorti, M., & Pieruccini, P. (2000). A late Lower Pliocene planation surface across the Italian Peninsula: a key tool in neotectonic studies. Journal of Geodynamics, 29(3-5), 323-328.

Costantini, M. (1998). A novel phase unwrapping method based on network programming. IEEE Transactions on geoscience and remote sensing, 36(3), 813-821.

Crosta, G., & Zanchi, A. (2000). Deep seated slope deformations: huge, extraordinary, enigmatic phenomena. In Bromhead, E., Dixon, N., Ibsen, M. (Eds.), Landslides in Research, Theory and Practice, Proceedings of the 8th International Symposium on Landslides Cardiff. Thomas Telford Publishing, 351-358.

Crosta, G.B., Frattini, P., & Agliardi, F. (2013). Deep seated gravitational slope deformations in the European Alps. Tectonophysics, 605, 13-33.

Deiana, G. (2009). Note Illustrative della Carta Geologica d'Italia alla scala 1: 50.000, Foglio 302 Tolentino.

Demangeot, J. (1965). Géomophologie des Abruzzes Adriatiques. Centre Recherche et Documentation Cartographiques Memoires et Documents, Numero hors serie, 1–403, Paris.

Devoti, R., Esposito, A., Pietrantonio, G., Pisani, A.R., & Riguzzi, F. (2011). Evidence of large scale deformation patterns from GPS data in the Italian subduction boundary. Earth and Planetary Science Letters, 311(3), 230-241.

Dramis, F., & Sorriso-Valvo, M. (1994). Deep-seated gravitational slope deformations, related landslides and tectonics. Engineering Geology, 38(3-4), 231-243.

Galadini, F. (2006). Quaternary tectonics and large-scale gravitational deformations with evidence of rock-slide displacements in the Central Apennines (central Italy). Geomorphology, 82(3-4), 201-228.

Goguel, J. (1978). Scale-dependent rockslide mechanisms, with emphasis on the role of pore fluid vaporization. In Voight, B. (Ed.), Developments in geo-technical engineering, 1978, 14a, Rockslides and avalanches, Elsevier, 693–705.

Goldstein, R. M., & Werner, C. L. (1998). Radar interferogram filtering for geophysical applications. Geophysical research letters, 25(21), 4035-4038.

Gori, S., Falcucci, E., Dramis, F., Galadini, F., Galli, P., Giaccio, B., Messima, P., Pizzi, A., Sposato, A. & Cosentino, D. (2014). Deep-seated gravitational slope deformation, large-scale rock failure, and active normal faulting along Mt. Morrone (Sulmona basin, Central Italy): geomorphological and paleoseismological analyses. Geomorphology, 208, 88-101.

Gutiérrez, F., Ortuño, M., Lucha, P., Guerrero, J., Acosta, E., Coratza, P., Piacentini, D. & Soldati, M. (2008). Late Quaternary episodic displacement on a sackung scarp in the central Spanish Pyrenees; secondary paleoseismic evidence?. Geodinámica Acta, 21(4), 187-202.

H. Brown Planation surface R.W. Fairbridge (Ed.), Encyclopaedia of Geomorphology, Reinhold, New York (1969)

Materazzi, M., Aringoli, D., Pambianchi, G., Gentili, B., & Giacopetti, M. (2015). Deep seated gravitational slope deformations and large landslides interfering with fluvial dynamics; examples from Central Apennines (Italy). In: Lollino, G., et al. (Eds.) Engineering Geology for Society and Territory, 2. Springer International Publishing Switzerland, 198–203.

McCalpin, J.P& Irvine, J.R. (1995). Sackungen at the Aspen Highlands ski area, Pitkin County, Colorado. Environmental & Engineering Geoscience, 1(3), 277-290.

McCalpin, J.P., & Hart, E.W. (2003). Ridge-top spreading features and relationship to earthquakes, San Gabriel Mountains region, Southern California; Part A. Distribution and description of ridge-top depressions (sackungen); Part B. Paleoseismic investigations of ridge-top depressions. In E.W. Hart (Ed.), Ridge-Top Spreading in California. California Geological Survey, Open-File Report, 1.

McCalpin, J.P., Bruhn, R.L., Pavlis, T.L., Gutierrez, F., Guerrero, J., & Lucha, P. (2011). Antislope scarps, gravitational spreading, and tectonic faulting in the western Yakutat microplate, south coastal Alaska. Geosphere, 7(5), 1143-1158.

Michele, M., Di Stefano, R., Chiaraluce, L., Cattaneo, M., De Gori, P., Monachesi, G., Latorre, D., Marzorati, S., Valoroso, L., Ladina, C., Chiarabba, C., Lauciani, V., Fares, M. (2016). The Amatrice 2016 seismic sequence: a preliminary look at the mainshock and aftershocks distribution. Annals of Geophysics, 59.

Miller, D.J., & Dunne, T. (1996). Topographic perturbations of regional stresses and consequent bedrock fracturing. Journal of Geophysical Research: Solid Earth, 101(B11), 25523-25536.

Moro, M., Chini, M., Saroli, M., Atzori, S., Stramondo, S., & Salvi, S. (2011). Analysis of large, seismically induced, gravitational deformations imaged by high-resolution COSMO-SkyMed synthetic aperture radar. Geology, 39(6), 527-530.

Moro, M., Saroli, M., Gori, S., Falcucci, E., Galadini, F., & Messina, P. (2012). The interaction between active normal faulting and large scale gravitational mass movements revealed by paleoseismological techniques: a case study from central Italy. Geomorphology, 151, 164-174.

Moro, M., Saroli, M., Salvi, S., Stramondo, S., & Doumaz, F. (2007). The relationship between seismic deformation and deep-seated gravitational movements during the 1997 Umbria–Marche (Central Italy) earthquakes. Geomorphology, 89(3), 297-307.

Pánek, T., & Klimeš, J. (2016). Temporal behavior of deep-seated gravitational slope deformations: a review. Earth-Science Reviews, 156, 14-38.

Polcari, M., Montuori, A., Bignami, C., Moro, M., Stramondo, S., & Tolomei, C. (2017). Using multi-band InSAR data for detecting local deformation phenomena induced by the 2016–2017 Central Italy seismic sequence. Remote Sensing of Environment, 201, 234-242. DOI: 10.1016/j.rse.2017.09.009

Radbruch-Hall, D.H. (1978). Gravitational creep of rock masses on slopes. In B. Voight (Ed.), Rockslide and Avalanches, 1, Elsevier, 607-657.

Raffy, J. (1979). Le Versant tyrrhénien de l'Apennin central (Doctoral dissertation). Paris-Sorbonne University.

Salvini, F. (2004). Daisy 3: The Structural Data Integrated System Analyzer Software: University of Roma Tre. Roma: http://host. uniroma3. it/progetti/fralab.

Small, R.J. (1978). The Study of Landforms. Cambridge University Press, Cambridge, 495 pp.

Tolomei, C., Taramelli, A., Moro, M., Saroli, M., Aringoli, D., & Salvi, S. (2013). Analysis of the deep-seated gravitational slope deformations over Mt. Frascare (Central Italy) with geomorphological assessment and DInSAR approaches. Geomorphology, 201, 281-292.

Varnes, D.J., Radbruch-Hall, D.H., Varnes, K.L., Smith, W.K., & Savage, W.Z. (1990). Measurement of ridge-spreading movements (Sackungen) at Bald Eagle Mountain, Lake County, Colorado, 1975-1989 (No. 90-543). U.S. Geological Survey Open-File Report, 90-543.

Werner, C., U. Wegmüller, T. Strozzi, and A. Wiesmann (2003). Interferometric point target analysis for deformation mapping, Geosci. Remote Sens. Symp., 7, 4362–4364, doi:10.1109/IGARSS.2003.1295516.